DNA-PKcs promotes DNA end processing

Authors: Rajashree A. Deshpande[1,2], Logan R. Myler[1,2], Michael M. Soniat[2], Linda Lee[3], Susan P. Lees-Miller[3], Ilya J. Finkelstein[2,4], and Tanya T. Paull[1, 2, *]

Affiliations: [1]The Howard Hughes Medical Institute and [2] the Department of Molecular Biosciences, The University of Texas at Austin, Austin, TX 78712 USA. [3] Department of Biochemistry and Molecular Biology, University of Calgary, Alberta, T2N 1N4, Canada. [4] The Center for Systems and Synthetic BIology, The University of Texas at Austin, Austin, TX 78712 USA.

*corresponding author, tpaull@utexas.edu

Abstract:

DNA-dependent Protein Kinase (DNA-PK) coordinates the repair of double-strand breaks through non-homologous end joining, the dominant repair pathway in mammalian cells. Breaks can also be resolved through homologous recombination during S/G_2 cell cycle phases, initiated by the Mre11-Rad50-Nbs1 (MRN) complex and CtIP-mediated resection of 5' strands. The functions of DNA-PK are considered to be end-joining specific, but here we demonstrate that human DNA-PK also plays an important role in the processing of DNA double-strand breaks. Using ensemble biochemistry and single-molecule approaches, we show that the MRN complex in cooperation with CtIP is stimulated by DNA-PK to perform efficient endonucleolytic processing of DNA ends in physiological conditions. This activity requires both CDK and ATR phosphorylation of CtIP. These unexpected results could explain the absence of DNA-PK deletion mutations in the human population, as homologous recombination is an essential process in mammals.

One sentence summary: An enzyme critical for non-homologous repair of DNA double-strand breaks also stimulates end processing for homologous recombination.

Main Text:

DNA-dependent Protein Kinase consists of a catalytic kinase subunit (DNA-PKcs) and the DNA end-binding heterodimer of Ku70 and Ku80 (Ku). Together, these proteins form an end recognition complex (DNA-PK) that binds to DNA double-strand breaks within seconds of break formation (*1*). DNA-PK promotes the ligation of two DNA ends by ligase IV, aided by the accessory factors XLF, XRCC4, and APLF, and in some cases aided by limited end processing (*1*, *2*). The recognition and repair of DNA breaks by the end-joining machinery is generally considered to be the first and rapid phase of DNA repair, occurring within ~30 minutes of DNA damage, while homologous recombination is specific to the S and G_2 phases of the cell cycle and occurs over a longer time frame (*3*, *4*). DNA-PK is present at micromolar concentrations in cells (*5*) and binds DNA ends in all cell cycle phases, even during S phase at single-ended breaks (*6*). The MRN complex regulates the initiation of DNA end processing prior to homologous recombination by catalyzing the initial 5' strand processing at blocked DNA ends and by recruiting long-range nucleases Exo1 and Dna2 (*4*, *7*). At single-ended breaks during replication, the nuclease activity of Mre11 was shown to be important for removal of Ku (*6*), suggesting that MRN catalytic processing of ends during S phase is important for recombination-mediated repair of single-ended breaks. While we and others have shown that MRN endonuclease activity is specifically stimulated by protein blocks on DNA ends (*8*–*11*), we considered the possibility that DNA-PK itself constitutes a powerful block to resection, and that DNA-PK may create a critical barrier to end processing at single-ended breaks where there is no other DNA end to participate in end joining.

To test for the effect of DNA-PKcs on end processing by Mre11, we performed a nuclease assay with recombinant human MRN, CtIP, Ku, and DNA-PKcs (Fig. S1) on a 197 bp linear double-stranded DNA containing a single radiolabel at the end of one of the 5′ strands. Addition of all the protein complexes together to this substrate resulted in the appearance of

single major cleavage product approximately 45nt in length (Fig. 1A, lane 2). We previously reported MRN removal of the Ku heterodimer alone, showing that MRN makes an endonucleolytic cleavage at approximately 30 bp from the DNA end (*12*); here we observe that the inclusion of DNA-PKcs in the reaction increases the efficiency of the cutting by ~50-fold as well as changing the position of the nuclease cleavage site to a location approximately 45 nt from the end (Fig. 1A, lanes 2 and 3). Formation of the cleavage product requires CtIP, which has been shown to promote the endonuclease activity of Mre11 on heterologous substrates (*8*, *9*). Mre11 nuclease activity in vitro is generally reported to be manganese-dependent; however, Mre11/Rad50 complexes from archaea and from T4 bacteriophage also exhibit nuclease activity in magnesium when physiologically relevant protein cofactors are present (*13*, *14*). Here we observe that human MRN makes endonucleolytic cuts in magnesium and that this requires the presence of both Ku and DNA-PKcs (Fig. 1A, lane 10). Since human cells do not contain high levels of manganese (*15*), we conclude that the physiologically relevant endonuclease activity of MRN is thus dependent on DNA-PK.

Mre11 and CtIP both exhibit endonucleolytic activity (*8*, *16*) so we asked which protein is responsible for the catalysis. DNA-PK-dependent cutting is completely absent when a nuclease-deficient form of Mre11(H129N) (*17*, *18*) is used in place of wild-type Mre11, whereas we see robust activity with nuclease-deficient N289A/H290A CtIP (Fig. 1B, lanes 4 and 5); thus, we conclude that the processing is done by the catalytic activity of Mre11. We have previously observed that ATP binding by Rad50 promotes Nbs1-dependent endonucleolytic cutting by Mre11 (*8*, *19*). Here we find that ATP is essential and the nonhydrolyzable AMP-PNP analog does not substitute for ATP in promoting MRN nuclease activity in the presence of DNA-PK (Fig. 1B, lanes 6 and 7). In the reactions shown in Fig. 1A and B, we have also included an inhibitor of DNA-PKcs, NU7441, to block its kinase activity since phosphorylation of Ku has been shown to result in the removal of Ku from DNA (*20*), and autophosphorylation of DNA-

PKcs also removes DNA-PKcs from the Ku-DNA complex (*21–25*). Removal of the inhibitor reduces the efficiency of the reaction (Fig. 1B, lane 8), indicating that kinase activity of DNA-PKcs is not required for Mre11 cutting, but the endonucleolytic product is still observed in the absence of the inhibitor so blocking DNA-PKcs phosphorylation is not essential.

We recently showed that MRN can remove DNA end blocks by sequential endo-exo-endo activities, generating a double-strand break adjacent to the block (*8*, *12*), a model first suggested by processing of meiotic DNA breaks (*26*). In the presence of DNA-PK bound to DNA ends, the MRN complex executes similar end-processing of the radiolabeled substrate. We detected a ~ 50 bp dsDNA product using native PAGE, corresponding to the major product seen on denaturing gels (Fig. 1C, lane 2). This activity was dependent on MRN and enhanced when both Ku and DNA-PKcs were present in the reaction (Fig. 1C, lanes 2 to 5). However, the formation of dsDNA cuts is less efficient compared to the single-strand endonucleolytic product seen on denaturing gels (Fig. 1A, B).

The unexpected dependence of Mre11 endonuclease activity on DNA-PK suggests that there may be specific protein-protein interactions underlying the cooperative behavior. We tested this by immobilizing purified, human CtIP on magnetic beads and testing for binding of DNA-PK or MRN. Both MRN and DNA-PK bind to CtIP in an ATP-independent manner (Fig. 1D). Binding analysis of Ku and DNA-PKcs separately showed that each of the components of DNA-PK has affinity for CtIP (Fig. 1E). Interestingly, binding of Nbs1 (which is added to this reaction separately from the MR complex) to CtIP is independent of DNA-PK while binding of MR to CtIP improves 7 to 8-fold with DNA-PK present. Addition of EtBr or Benzonase to the reaction did not affect the interaction, confirming that the binding is independent of DNA (Fig. S2).

Exo1 is one of the critical long-range exonucleases that performs DNA end resection in human cells (*4*) and we have previously shown a positive effect of MRN on Exo1-mediated degradation of DNA (*27*, *28*). Despite the well-known importance of CtIP in resection in human cells, however, we have not observed any effects of recombinant CtIP on Exo1 activity in previous experiments (data not shown). Here we examined the effect of CtIP on Exo1 on a plasmid DNA substrate in the presence of MRN and DNA-PK, finding that CtIP stimulates the activity of Exo1 7-fold in the presence of DNA-PK, consistent with its effect on Mre11 nuclease activity we observe on the labeled substrates (Fig. 1F).

CtIP is phosphorylated by several different kinases in human cells (*29*)(Fig. 2A). Some of these phosphorylation events have been shown to promote DNA end resection in cells (*8*, *9*, *30*–*35*), most notably the CDK-dependent modification of T847. In addition, ATR phosphorylation of T859 also plays an important role in CtIP binding to chromatin and CtIP-mediated resection (*36*). We tested the role of CtIP phosphorylation by purifying phospho-blocking and phospho-mimic mutants at these sites (Fig. S1). Addition of these proteins to the MRN endonuclease assay with DNA-PK shows that T847 and T859 phosphorylation are critical, as the phospho-deficient T847A and T859A mutants resulted in loss of CtIP stimulation (15 and 3 fold stimulation of MRN, respectively, compared to 43 fold-by WT) (Fig. 2B, lanes 5-10, Fig. 2C). In contrast, phosphorylation at S327 or the ATM sites S231, S664 and S745 appears not to be essential for the endonucleolytic activity (Fig. 2B, lanes 11-13). We previously found that the ATM phosphorylation sites are important for CtIP intrinsic nuclease activity (*37*). Here we show that these sites do not regulate DNA-PK-dependent Mre11 endonuclease activity, consistent with our observation that the N289A/H290A mutations that reduce CtIP nuclease activity also do not impact Mre11 function in this assay.

While mutation of the CtIP T847 residue to phospho-blocking alanine inhibits its stimulation of Mre11 nuclease activity, the phospho-mimic T847E mutant completely restores

this ability in vitro (Fig. 2C, lane 6). This is important as the T847E allele of CtIP was shown previously to restore localization of CtIP to sites of DNA damage as well as the resection of double-strand breaks, and promoted efficient CDK-independent processing of these breaks (*33*). Thus the phosphorylation of T847 in CtIP links Mre11 endonuclease activity to the cell cycle-dependent processing of DNA damage. The T859E phospho-mimic version of CtIP only partially restores Mre11 activity (Fig. 2B, lane 8), also consistent with the initial study of T859 phosphorylation by ATR in Xenopus extracts which reported that the T859E (T818E in Xenopus CtIP) is only weakly active in supporting double-strand break resection in CtIP-depleted extracts (*36*).

To examine the interactions between DNA-PK and the MRN complex in greater detail, we turned to single-molecule microscopy. In this "DNA curtains" assay, arrays of lambda DNA molecules (~48 kb long) are attached via a biotin-streptavidin linkage to a microfluidic flowcell that is also passivated with a fluid lipid bilayer (Fig. 3A). (*38*). Microfabricated barriers align the DNA molecules and organize them for high throughput analysis of bound proteins, which we have previously used to examine the interplay between the MRN complex and Ku at individual DNA ends (*12*). Here we adapted this assay to observe the behavior of the DNA-PK complex, with DNA-PKcs labeled using a DNA-PKcs-specific antibody. Injection of fluorescently labeled DNA-PKcs led to only transient association with the DNA, as indicated by non-specific sliding in the direction of buffer flow and subsequent release from the DNA ends (half-life = 5 ± 3 sec, N=17; Fig. 3B). Given that formation of the DNA-PK complex requires Ku and DNA (*39*), we considered that pre-loaded Ku may stabilize DNA-PKcs on the DNA ends. To test this, we injected HA-tagged Ku heterodimer onto the DNA curtains, labeled with anti-HA antibody. As we observed previously, Ku binds only to DNA ends and does not slide on the DNA with buffer flow (*12*). Subsequent injection of DNA-PKcs did result in more stable association of the kinase with the Ku-bound ends; however, the inclusion of ATP in the buffer promoted rapid loss of ~50% of

the bound Ku molecules (data not shown). These are single-turnover reactions that we observe with constant buffer flow, so even transient release of DNA-PKcs from the DNA results in loss of association. We considered that the ATP-dependent release might be associated with the phosphorylation of Ku70 by DNA-PKcs, which was reported to inhibit DNA binding by Ku (*20*). To prevent Ku phosphorylation and release by DNA-PKcs, we purified a phospho-blocking mutant of Ku(T305A/S306A/T307A/S314A/T316A, "5A"), which was reported to inhibit DNA-PKcs-induced Ku release (*20*). Ku(5A) bound to DNA for >2000 seconds, consistent with our previous observations of extremely stable binding of wild-type Ku (Fig. 3C)(*12*). Injection of DNA-PKcs onto Ku(5A)-bound DNA curtains led to a stabilization of DNA-PKcs on the Ku-bound DNA ends (Fig. 3C,D), suggesting that the phosphorylation of the S/TQ 305-316 cluster of sites on Ku70 does control the association of both the Ku heterodimer as well as the DNA-PKcs kinase.

We next observed the interplay between MRN and DNA-PK (DNA-PKcs with Ku(5A)) using the DNA curtains platform. Consistent with our ensemble biochemical assays, injection of dark MRN and CtIP onto DNA curtains with both DNA-PKcs and Ku labeled in the presence of a physiologically relevant cleavage buffer (5 mM Mg^{2+}) led to removal of both DNA-PKcs and Ku from the ends (Fig. 4A). In order to probe the dynamics of this activity, we utilized fluorescently-labeled MRN complex together with labeled DNA-PKcs (Ku is unlabeled in this case) and measured the occupancy of DNA-PK on ends that are also bound by MRN. Injection of MRN alone led to stable co-localization of the two complexes (DNA-PK half-life >2000 sec), but injection of MRN and CtIP together led to removal of both Ku and DNA-PKcs from the DNA ends (half-life = 324 ± 15 sec, N=37; Fig. 4B and Fig. 4C). In contrast, an MRN nuclease-deficient mutant (H129N) with CtIP did not remove DNA-PK, neither did CtIP added in the absence of MRN. Furthermore, injection of MRN with CtIP containing phospho-blocking mutations T847A and T859A also failed to remove DNA-PK (Fig. 4C), suggesting that co-

localization of MRN with the DNA-PK complex is not sufficient to facilitate removal and that, consistent with our biochemical assays, phosphorylated CtIP is required for DNA-PK stimulation of MRN nuclease activity.

Our previous studies of MRN and Ku dynamics on DNA ends using the DNA curtains system and ensemble assays showed MRN cleavage of Ku alone, but this reaction required manganese ions (*8*, *12*). Other studies also recently demonstrated yeast Mre11/Rad50/Xrs2(MRX) cleavage of various protein blocks including yeast Ku, which was also manganese-dependent in vitro (*10*, *11*). Here we observe approximately the same kinetics of DNA-PK release catalyzed by MRN and CtIP as we did previously, but in magnesium-only conditions. These results demonstrate that Mre11 nuclease activity can act in the absence of manganese with relevant protein cofactors. Both Ku and DNA-PKcs appear to be released from the DNA, suggesting the creation of a clean double-strand break.

In conclusion, we have shown that DNA-PK plays an important role in DNA end processing through its stimulation of Mre11 endonuclease activity. The extremely high concentration of DNA-PK in mammalian cells, particularly in human cells (*5*), means that double-strand break ends will be bound with DNA-PK (see model in Fig. 4D). Removal of this block can be promoted by several distinct mechanisms: by DNA-PKcs phosphorylation of Ku70 which reduces its DNA-binding affinity (*20*), by ubiquitination of Ku and degradation by proteasome-dependent or independent mechanisms (*40–42*), and, as we show in this study, by Mre11-mediated catalytic removal and DNA end cleavage. Mre11 activity on DNA-PK-bound ends is promoted by stable occupancy of DNA-PK on the ends, as shown by the increased efficiency of MRN cleavage in the presence of the DNA-PK inhibitor, which prevents autophosphorylation and dissociation (*1*). This requirement for stable occupancy of DNA-PK ensures that MRN does not cleave ends which are undergoing successful end-joining, as this outcome also leads to DNA-PKcs dissociation (*43*). DNA-PK and MRN have often been viewed

as competitors for DNA ends, but the data presented here shows that these complexes are linked in an ordered pathway. The dual roles of DNA-PKcs ensure rapid repair by NHEJ then also promote an efficient transition to homologous recombination by promoting DNA-PK removal and the initiation of end processing.

The requirement for DNA-PKcs in promoting human MRN-mediated end processing may account for some of the differences between human and rodent cell lines deficient in DNA-PK components (*44*). Mice lacking DNA-PKcs are developmentally normal apart from a deficiency in V(D)J and class switch recombination (*45*), while no human individuals have been identified with a complete loss of DNA-PKcs. A recently identified patient with very little functional DNA-PKcs due to rare mutations in the *PRKDC* gene exhibited severe growth defects and neurological impairment (*46*). The severe nature of this phenotype suggest that complete loss of DNA-PKcs is lethal in humans. A role for human DNA-PKcs in homologous recombination would certainly be consistent with this conclusion, as core factors necessary for homologous recombination are essential (*47*).

Materials and Methods:

Plasmid, strains and Protein purification

Wild-type hMR, hMRN and hM(H129N)RN complexes, and Nbs1 were expressed and purified from Sf21 insect cells as described previously (*8*). CtIP wild-type and mutant proteins were expressed and purified from Sf21 cells as described previously (*37*). 3XFLAG-MRN, 3XHA-Ku70/80 heterodimer, and Exo1-biotin were made as described previously (*12*). DNA-PKcs from human cells was purified as described previously (*48*). The Ku70(5A) mutant (T305A/S306A/T307A/S314A/T316A) was made from the baculovirus transfer vector containing wild-type Ku70 by QuikChange mutagenesis (Stratagene) to create the 5A mutant expression

plasmid pTP4143 and the corresponding bacmid pTP4177, which was used with wild-type Ku80 baculovirus to infect Sf21 cells and purify Ku(5A).

DNA substrates

TP542 (GGTTTTCCCAGTCACGACGTTG) was 5′ [^{32}P] radiolabeled using T4 polynucleotide kinase (NEB) and purified (NEB Nucleotide Removal Kit). The 197 bp DNA substrate labeled on the 5′ end was created by PCR using 5' [^{32}P] radiolabeled TP542 (GGTTTTCCCAGTCACGACGTTG) and TP4373(TGGGTCAACGTGGGCAAAGATGTCCTAGCAATGTAATCGTCTATGACGTT) with pTP3718 followed by purification on a native 0.7% agarose gel as described previously (*8*). The DNA substrate used in Figure 1F was made by digesting pCDF-1b plasmid with SspI to create a 3.6 kb linear DNA with blunt ends, and was used without further purification. The lambda DNA substrate used in single molecule studies was prepared as described previously (*12*).

Nuclease assays

10 µl nuclease assays contained Ku70/80 (10 nM), DNA-PKcs (10 nM), hMR (50 nM), Nbs1 (50 nM) and CtIP (80 nM) unless indicated otherwise in figure legends. Reactions were performed with 0.1 nM DNA in 25 mM MOPS pH 7.0, 20 mM Tris pH 8.0, 80 mM NaCl, 8 % glycerol, 1 mM DTT, 1 mM ATP, 0.2 mM NU7441, 5 mM $MgCl_2$, 1 mM $MnCl_2$ and 0.2 mg/ml BSA, with additions or exceptions as noted in the figures and legends. hMR and Nbs1 were pre-incubated (10 min. at 4 °C) prior to addition to reactions, and Ku and DNA-PKcs were allowed to bind DNA in the presence of NU7441 for 5 min. at 25 °C followed by the addition of other components. Assays were carried out in Protein Lo-Bind eppendorf tubes (Millipore) at 37°C for 30 min. Reactions were stopped with 0.2 % SDS and 10 mM EDTA, lyophilized, dissolved in formamide, boiled at 100°C for 4 min, loaded on denaturing polyacrylamide gels containing 16% acrylamide,

20% formamide and 6M urea, and separated at 40W for 1.5 h, followed by phosphorimager analysis. For the detection of dsDNA products, reactions were treated with 10 µg Proteinase K at 37°C for 1h after stopping the nuclease reaction. The samples were then separated using 12% native PAGE in 1X Tris-Borate-EDTA (TBE) buffer at 150V followed by phosphorimager analysis.

DNA resection assays on plasmid substrates were carried out similarly using 0.1 nM 3.6 kb pCDF-1b plasmid linearized with SspI and 1 nM Exo1 in the presence of the DNA-PKcs inhibitor NU7026 (200 µM). Reactions were stopped with 0.2 % SDS and 10 mM EDTA, 1.5 µg Proteinase K was added and incubated at 37°C for 90 min followed by 10 min incubation at 50°C. These reactions were separated in a 0.7% native agarose gel in 1X TBE buffer, stained with SYBR green and visualized with a Chemidoc Gel Imager (Bio-Rad).

Protein- protein interactions

Immunoprecipitation assays were performed with anti-CtIP antibody (Active Motif 14E1) in Protein Lo-Bind eppendorf tubes (Millipore). In a 40 µl reaction volume, 20 nM Ku70/80, 20 nM DNA-PKcs, 25 nM hMR, 25 nM Nbs1 and 16 nM CtIP were incubated as indicated in the absence of DNA in 25 mM MOPS pH 7.0, 20 mM Tris, pH 8.0, 80 mM NaCl, 8 % glycerol, 1 mM DTT, 1 mM ATP, 0.2 mM NU7441, 5 mM $MgCl_2$ and 0.2 mg/ml BSA at 37°C for 10 min. The reaction was then incubated with 2 µg anti-CtIP antibody, 0.4% 3-[(3-Cholamidopropyl)dimethylammonio]-1-propanesulfonate (CHAPS) and 2 µl Protein A/G magnetic beads (Pierce) at 37°C for 30 min with shaking. Beads were isolated using a magnet and washed 3 times with wash buffer (Buffer A (25 mM Tris pH 8.0, 100 mM NaCl, 10% glycerol) containing 0.4% CHAPS and 0.1 mg/ml BSA). Tubes were changed at the third wash step and proteins bound to the beads were eluted with 1X SDS-PAGE loading dye prepared in wash buffer. Samples were heated at 100°C for 5 min and separated by 8% SDS-PAGE

followed by Western blotting. Since Mre11 and Ku80 migrate very close to each other, blots were developed sequentially, first for FLAG tagged CtIP, Nbs1 and Mre11, then for DNA-PKcs and His tagged Rad50 and Ku70, and lastly for biotin-tagged Ku80. Proteins were detected using rabbit anti-FLAG (Cell Signaling), rabbit anti-DNA-PKcs (Bethyl Laboratories), and mouse anti-His (Genscript) antibodies as well as streptavidin-Alexa Fluor680 conjugate (Invitrogen) using an Odyssey Imager (Li-Cor).

Single molecule experiments

Single-molecule DNA curtains were performed as previously described (*12*). For labeling of DNA-PKcs, 400 nM anti-mouse secondary QDots (Fisher) were incubated with 360 nM anti-DNA-PKcs antibody (Abcam) on ice for 10 minutes in 5 µl DNA-PKcs loading buffer (40 mM Tris-HCl pH 8.0, 0.2 mg/ml BSA, 2 mM $MgCl_2$, 2 mM DTT). DNA-PKcs was added to this mixture to for a final concentration of 267 nM QDots, 240 nM antibody, and 167 nM DNA-PKcs in 7.5 µl for another 10 minutes on ice. This mixture was diluted to a final volume of 200 µl (10 nM QDots, 9 nM antibody, 6.25 nM DNA-PKcs). Ku(5A) was loaded on DNA curtains essentially as described previously for wild-type Ku (*12*). Next, DNA-PKcs was injected onto DNA curtains from a 100 µl loop at 200 µl/min in DNA-PKcs loading buffer. For MRN cleavage experiments, after DNA-PKcs loading the buffer was switched to MRN cleavage buffer (40 mM Tris-HCl pH 8.0, 60 mM NaCl, 0.2 mg/mlBSA, 5 mM $MgCl_2$, 1 mM ATP, 2 mM DTT). After buffer switch, mixtures of 3 nM MRN, 14 nM CtIP, or both were loaded as previously described (*12*).

Acknowledgements:

We thank members of the Paull laboratory for useful discussions and for critically reading the manuscript. This work was supported by the National Institute of General Medical Sciences of the National Institutes of Health (GM120554 to I.J.F.), the National Cancer Institute of the National Institutes of Health (CA092584 to I.J.F. and S.P.L.M.), CPRIT (R1214 to I.J.F.,

RP110465 to T.T.P.), and the Welch Foundation (F-I808 to I.J.F.). I.J.F. is a CPRIT Scholar in Cancer Research. L.R.M. is supported by the National Cancer Institute of the National Institutes of Health (F99CA212452). M.M.S. is supported by a Postdoctoral Fellowship, PF-17-169-01-DMC, from the American Cancer Society. The content is solely the responsibility of the authors and does not necessarily represent the official views of the National Institutes of Health.

References

1. N. Jette, S. P. Lees-Miller, The DNA-dependent protein kinase: A multifunctional protein kinase with roles in DNA double strand break repair and mitosis. *Prog Biophys Mol Biol*. **117**, 194–205 (2015).

2. H. H. Y. Chang, N. R. Pannunzio, N. Adachi, M. R. Lieber, Non-homologous DNA end joining and alternative pathways to double-strand break repair. *Nat. Rev. Mol. Cell Biol.* **18**, 495–506 (2017).

3. A. A. Goodarzi, P. A. Jeggo, The repair and signaling responses to DNA double-strand breaks. *Adv Genet*. **82**, 1–45 (2013).

4. L. S. Symington, Mechanism and regulation of DNA end resection in eukaryotes. *Crit Rev Biochem Mol Biol*. **51**, 195–212 (2016).

5. T. Blunt *et al.*, Defective DNA-dependent protein kinase activity is linked to V(D)J recombination and DNA repair defects associated with the murine scid mutation. *Cell*. **80**, 813–823 (1995).

6. P. Chanut, S. Britton, J. Coates, S. P. Jackson, P. Calsou, Coordinated nuclease activities counteract Ku at single-ended DNA double-strand breaks. *Nat Commun*. **7**, 12889 (2016).

7. T. Aparicio, R. Baer, J. Gautier, DNA double-strand break repair pathway choice and cancer. *DNA Repair Amst*. **19**, 169–75 (2014).

8. R. A. Deshpande, J. H. Lee, S. Arora, T. T. Paull, Nbs1 Converts the Human Mre11/Rad50 Nuclease Complex into an Endo/Exonuclease Machine Specific for Protein-DNA Adducts. *Mol. Cell*. **64**, 593–606 (2016).

9. R. Anand, L. Ranjha, E. Cannavo, P. Cejka, Phosphorylated CtIP Functions as a Co-factor of the MRE11-RAD50-NBS1 Endonuclease in DNA End Resection. *Mol Cell*. **64**, 940–950 (2016).

10. G. Reginato, E. Cannavo, P. Cejka, Physiological protein blocks direct the Mre11-Rad50-Xrs2 and Sae2 nuclease complex to initiate DNA end resection. *Genes Dev*. **31**, 2325–2330 (2017).

11. W. Wang, J. M. Daley, Y. Kwon, D. S. Krasner, P. Sung, Plasticity of the Mre11-Rad50-Xrs2-Sae2 nuclease ensemble in the processing of DNA-bound obstacles. *Genes Dev*. **31**, 2331–2336 (2017).

12. L. R. Myler *et al.*, Single-Molecule Imaging Reveals How Mre11-Rad50-Nbs1 Initiates DNA Break Repair. *Mol. Cell*. **67**, 891-898 e4 (2017).

13. T. J. Herdendorf, D. W. Albrecht, S. J. Benkovic, S. W. Nelson, Biochemical characterization of bacteriophage T4 Mre11-Rad50 complex. *J Biol Chem*. **286**, 2382–92 (2011).

14. B. Hopkins, T. T. Paull, The P. furiosus Mre11/Rad50 complex promotes 5’ strand resection at a DNA double-strand break. *Cell*. **135**, 250–260 (2008).

15. A. B. Bowman, M. Aschner, Considerations on manganese (Mn) treatments for in vitro studies. *NeuroToxicology*. **41**, 141–142 (2014).

16. N. Makharashvili *et al.*, Catalytic and Noncatalytic Roles of the CtIP Endonuclease in Double-Strand Break End Resection. *Mol Cell* (2014), doi:10.1016/j.molcel.2014.04.011.

17. S. Moreau, J. R. Ferguson, L. S. Symington, The nuclease activity of Mre11 is required for meiosis but not for mating type switching, end joining, or telomere maintenance. *Mol Cell Biol*. **19**, 556–66 (1999).

18. J. Buis *et al.*, Mre11 nuclease activity has essential roles in DNA repair and genomic stability distinct from ATM activation. *Cell*. **135**, 85–96 (2008).

19. T. T. Paull, M. Gellert, Nbs1 potentiates ATP-driven DNA unwinding and endonuclease cleavage by the Mre11/Rad50 complex. *Genes Dev*. **13**, 1276–88 (1999).

20. K. J. Lee *et al.*, Phosphorylation of Ku dictates DNA double-strand break (DSB) repair pathway choice in S phase. *Nucleic Acids Res*. **44**, 1732–45 (2016).

21. W. D. Block *et al.*, Autophosphorylation-dependent remodeling of the DNA-dependent protein kinase catalytic subunit regulates ligation of DNA ends. *Nucleic Acids Res*. **32**, 4351–7 (2004).

22. Y. V. Reddy, Q. Ding, S. P. Lees-Miller, K. Meek, D. A. Ramsden, Non-homologous end joining requires that the DNA-PK complex undergo an autophosphorylation-dependent rearrangement at DNA ends. *J Biol Chem*. **279**, 39408–13 (2004).

23. Q. Ding *et al.*, Autophosphorylation of the catalytic subunit of the DNA-dependent protein kinase is required for efficient end processing during DNA double-strand break repair. *Mol Cell Biol*. **23**, 5836–48 (2003).

24. D. W. Chan *et al.*, Autophosphorylation of the DNA-dependent protein kinase catalytic subunit is required for rejoining of DNA double-strand breaks. *Genes Dev*. **16**, 2333–8 (2002).

25. N. Uematsu *et al.*, Autophosphorylation of DNA-PKCS regulates its dynamics at DNA double-strand breaks. *J Cell Biol*. **177**, 219–29 (2007).

26. V. Garcia, S. E. Phelps, S. Gray, M. J. Neale, Bidirectional resection of DNA double-strand breaks by Mre11 and Exo1. *Nature*. **479**, 241–4 (2011).

27. L. R. Myler *et al.*, Single-molecule imaging reveals the mechanism of Exo1 regulation by single-stranded DNA binding proteins. *Proc Natl Acad Sci U A*. **113**, E1170-9 (2016).

28. M. L. Nicolette *et al.*, Mre11-Rad50-Xrs2 and Sae2 promote 5' strand resection of DNA double-strand breaks. *Nat Struct Mol Biol*. **17**, 1478–85 (2010).

29. N. Makharashvili, T. T. Paull, CtIP: A DNA damage response protein at the intersection of DNA metabolism. *DNA Repair Amst*. **32**, 75–81 (2015).

30. T. Aparicio, R. Baer, M. Gottesman, J. Gautier, MRN, CtIP, and BRCA1 mediate repair of topoisomerase II-DNA adducts. *J Cell Biol*. **212**, 399–408 (2016).

31. K. Nakamura *et al.*, Collaborative action of Brca1 and CtIP in elimination of covalent modifications from double-strand breaks to facilitate subsequent break repair. *PLoS Genet*. **6**, e1000828 (2010).

32. F. Polato *et al.*, CtIP-mediated resection is essential for viability and can operate independently of BRCA1. *J. Exp. Med.* **211**, 1027–1036 (2014).

33. P. Huertas, S. P. Jackson, Human CtIP mediates cell cycle control of DNA end resection and double strand break repair. *J Biol Chem*. **284**, 9558–65 (2009).

34. M. H. Yun, K. Hiom, CtIP-BRCA1 modulates the choice of DNA double-strand-break repair pathway throughout the cell cycle. *Nature*. **459**, 460–3 (2009).

35. O. Barton *et al.*, Polo-like kinase 3 regulates CtIP during DNA double-strand break repair in G1. *J Cell Biol*. **206**, 877–94 (2014).

36. S. E. Peterson *et al.*, Activation of DSB Processing Requires Phosphorylation of CtIP by ATR. *Mol. Cell* (2012), doi:10.1016/j.molcel.2012.11.020.

37. N. Makharashvili *et al.*, Catalytic and noncatalytic roles of the CtIP endonuclease in double-strand break end resection. *Mol. Cell*. **54**, 1022–1033 (2014).

38. I. F. Gallardo *et al.*, High-Throughput Universal DNA Curtain Arrays for Single-Molecule Fluorescence Imaging. *Langmuir*. **31**, 10310–10317 (2015).

39. T. M. Gottlieb, S. P. Jackson, The DNA-dependent protein kinase: requirement for DNA ends and association with Ku antigen. *Cell*. **72**, 131–42 (1993).

40. L. Postow, Destroying the ring: Freeing DNA from Ku with ubiquitin. *FEBS Lett.* **585**, 2876–2882 (2011).

41. N. Jiang *et al.*, Valosin-containing protein regulates the proteasome-mediated degradation of DNA-PKcs in glioma cells. *Cell Death Dis.* **4**, e647 (2013).

42. J. van den Boom *et al.*, VCP/p97 Extracts Sterically Trapped Ku70/80 Rings from DNA in Double-Strand Break Repair. *Mol. Cell*. **64**, 189–198 (2016).

43. J.-S. Kim *et al.*, Independent and sequential recruitment of NHEJ and HR factors to DNA damage sites in mammalian cells. *J. Cell Biol.* **170**, 341–347 (2005).

44. B. L. Ruis, K. R. Fattah, E. A. Hendrickson, The catalytic subunit of DNA-dependent protein kinase regulates proliferation, telomere length, and genomic stability in human somatic cells. *Mol. Cell. Biol.* **28**, 6182–6195 (2008).

45. G. E. Taccioli *et al.*, Targeted disruption of the catalytic subunit of the DNA-PK gene in mice confers severe combined immunodeficiency and radiosensitivity. *Immunity*. **9**, 355–366 (1998).

46. L. Woodbine *et al.*, PRKDC mutations in a SCID patient with profound neurological abnormalities. *J. Clin. Invest.* **123**, 2969–2980 (2013).

47. M. E. Moynahan, M. Jasin, Mitotic homologous recombination maintains genomic stability and suppresses tumorigenesis. *Nat. Rev. Mol. Cell Biol.* **11**, 196–207 (2010).

48. D. W. Chan, C. H. Mody, N. S. Ting, S. P. Lees-Miller, Purification and characterization of the double-stranded DNA-activated protein kinase, DNA-PK, from human placenta. *Biochem. Cell Biol. Biochim. Biol. Cell.* **74**, 67–73 (1996).

Figure Legends

Figure 1: Nucleolytic removal of DNA-PK by MRN and its stimulation by CtIP.

(A) Nuclease reactions were performed with a 197 bp DNA substrate, 5' labeled with ^{32}[P](asterisk), with MRN (50 nM), CtIP (80 nM), Ku (10 nM), and DNA-PKcs (10 nM) as indicated, in the presence of both magnesium and manganese (lanes 1-8) or magnesium only (lanes 9-16). All reactions contained the DNA-PKcs inhibitor NU7441. Products were visualized by denaturing polyacrylamide gel electrophoresis and visualized by phosphorimager. Red and black arrows indicate the predominant product in the presence of DNA-PKcs and Ku, or Ku alone, respectively. (B) Nuclease assays were performed as in (A) in the presence of both magnesium and manganese with wild-type MRN or MRN containing nuclease-deficient Mre11 (H129N). Reactions without ATP or with AMP-PNP instead of ATP are indicated, as is the reaction without NU7441. (C) Double-stranded DNA cleavage products from the MRN nuclease assay with DNA-PK and CtIP were detected on a 12% native polyacrylamide gel. The red arrow indicates the ~45 bp product. (D) Protein-protein interactions between CtIP, MRN, and DNA-PK were measured by immunoprecipitation with anti-CtIP antibody in the presence or absence of ATP followed by western blotting of bound proteins, as indicated. (E) Interactions between CtIP, MRN, DNA-PKcs and Ku was measured with CtIP immunoprecipitation as in (D) in the presence of ATP. (F) DNA end resection on a plasmid substrate (3.6 kb) was performed with MRN, CtIP, DNA-PK, and Exo1 as indicated. Reaction products were separated in a native agarose gel, which was stained with SYBR green.

Figure 2: Stimulation of MRN nuclease activity by CtIP requires CtIP phosphorylation.

(A) A linear map of CtIP indicating a subset of known phosphorylated residues as well as residues important for DNA binding and catalytic activity as discussed in the text. (B) Nuclease assays were performed with MRN (12.5 nM), CtIP (40 nM), Ku (10 nM) and DNA-PK (10 nM) as

in Fig. 1A but with various mutants of CtIP as indicated, in the presence of both magnesium and manganese. The red arrow indicates the predominant product formed in the presence of DNA-PKcs. (C) Nuclease assays were performed as in (B) with titrations of CtIP (10, 20 and 40 nM).

Figure 3: Single-molecule visualization of DNA-PK on DNA

(A) Schematic of the DNA curtains assay for DNA-PK. (B) Illustration and kymograph of DNA-PKcs injection onto DNA curtains. White arrow indicates a single DNA-PKcs binding event. This molecule then slides along the DNA in the direction of buffer flow to reach the DNA end (green arrow). The molecule then associates for a short time at the end (t_e) before dissociation (red arrow). (C) Lifetime of Ku or DNA-PKcs on DNA curtains in the presence of DNA-PKcs and ATP. DNA-PKcs alone (blue), Ku(5A) alone (red) or Ku(5A) plus DNA-PKcs (green) were injected onto DNA curtains and the lifetime of DNA-PKcs (or Ku in the case of Ku(5A) added alone) was monitored. Half-lives of each complex are as indicated (n=70, 17, and 66, respectively). (D) Illustration and kymographs of DNA-PKcs sliding to co-localize with an end-bound Ku(5A).

Figure 4. DNA-PKcs occupancy at single ended DNA double-strand break is regulated by Mre11 nuclease activity.

(A) Illustration and kymographs of DNA-PKcs (magenta) and Ku (green) upon injection of MRN (dark) and CtIP (dark). (B) Kymographs of DNA-PKcs (magenta) with Ku (dark), with injection of MRN (green) alone (top), or MRN with CtIP (middle), or a nuclease-dead mutant of MRN (H129N) with CtIP (bottom). (C) Lifetimes and associated half-lifes of the DNA-PK complex (as observed by DNA-PKcs occupancy) upon no injection (green), injection with with MRN and CtIP (black), MRN alone (red), nuclease deficient H129N MRN and CtIP (magenta), CtIP only (blue), or MRN with phospho-blocking T847A/T859A CtIP (purple). (D) Model for MRN recognition of DNA-bound DNA-PK showing the stimulation of MRN endonucleolytic cleavage of the end in the

presence of phosphorylated CtIP. MRN also promotes the long-range resection activity of Exo1 through interactions with Exo1 that prevent inhibition by RPA (*27*).

Figure 1

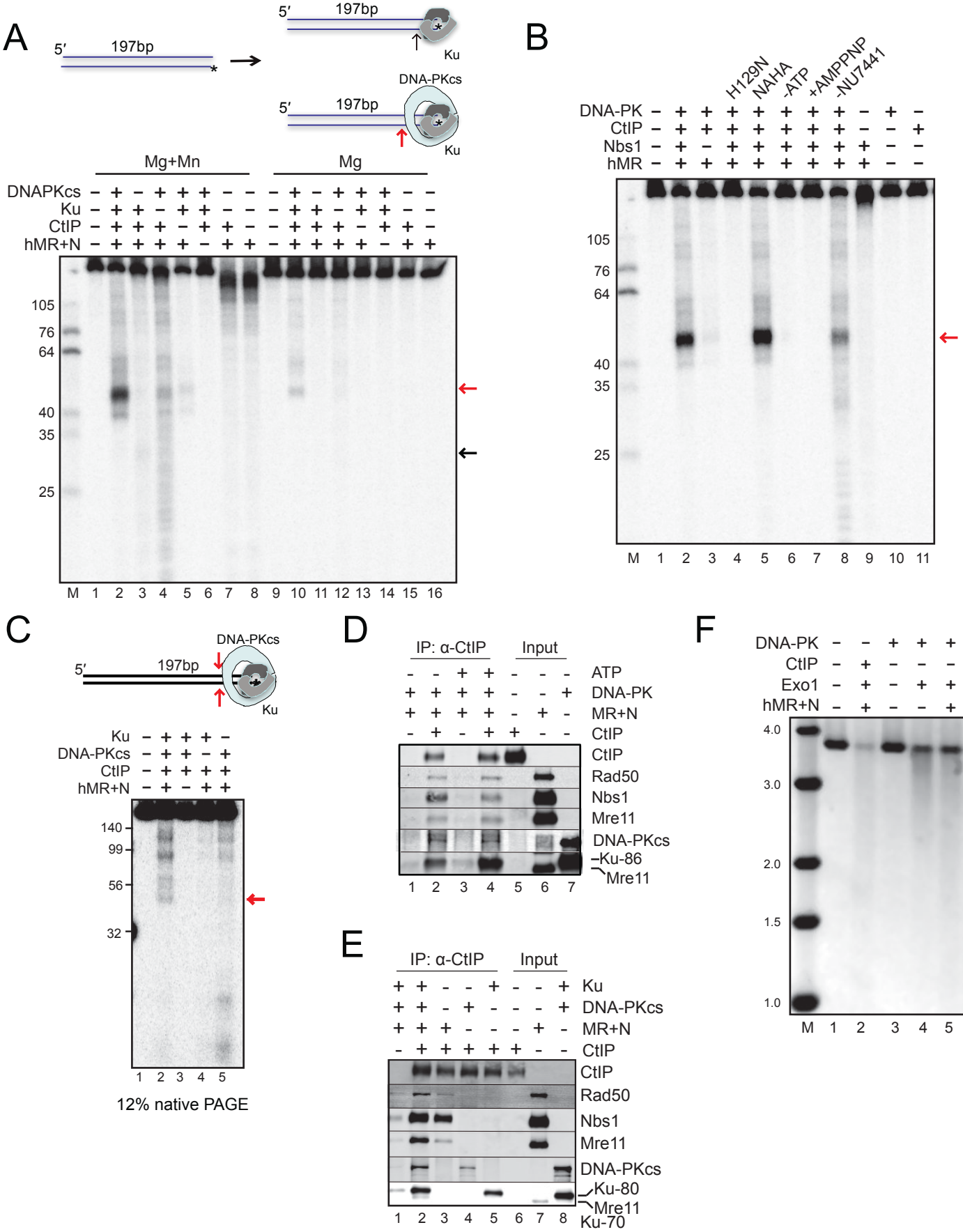

Figure 2

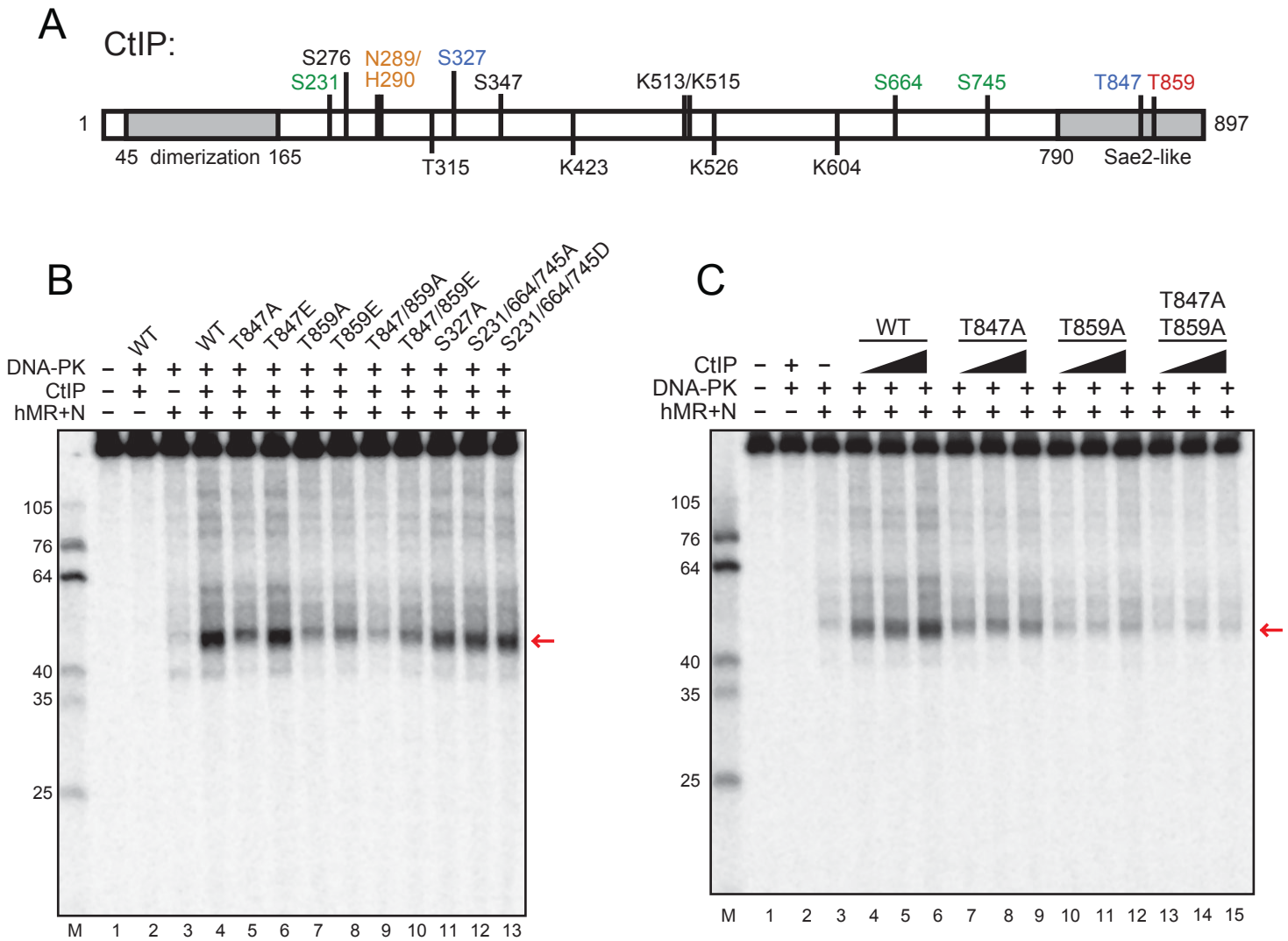

Figure 3

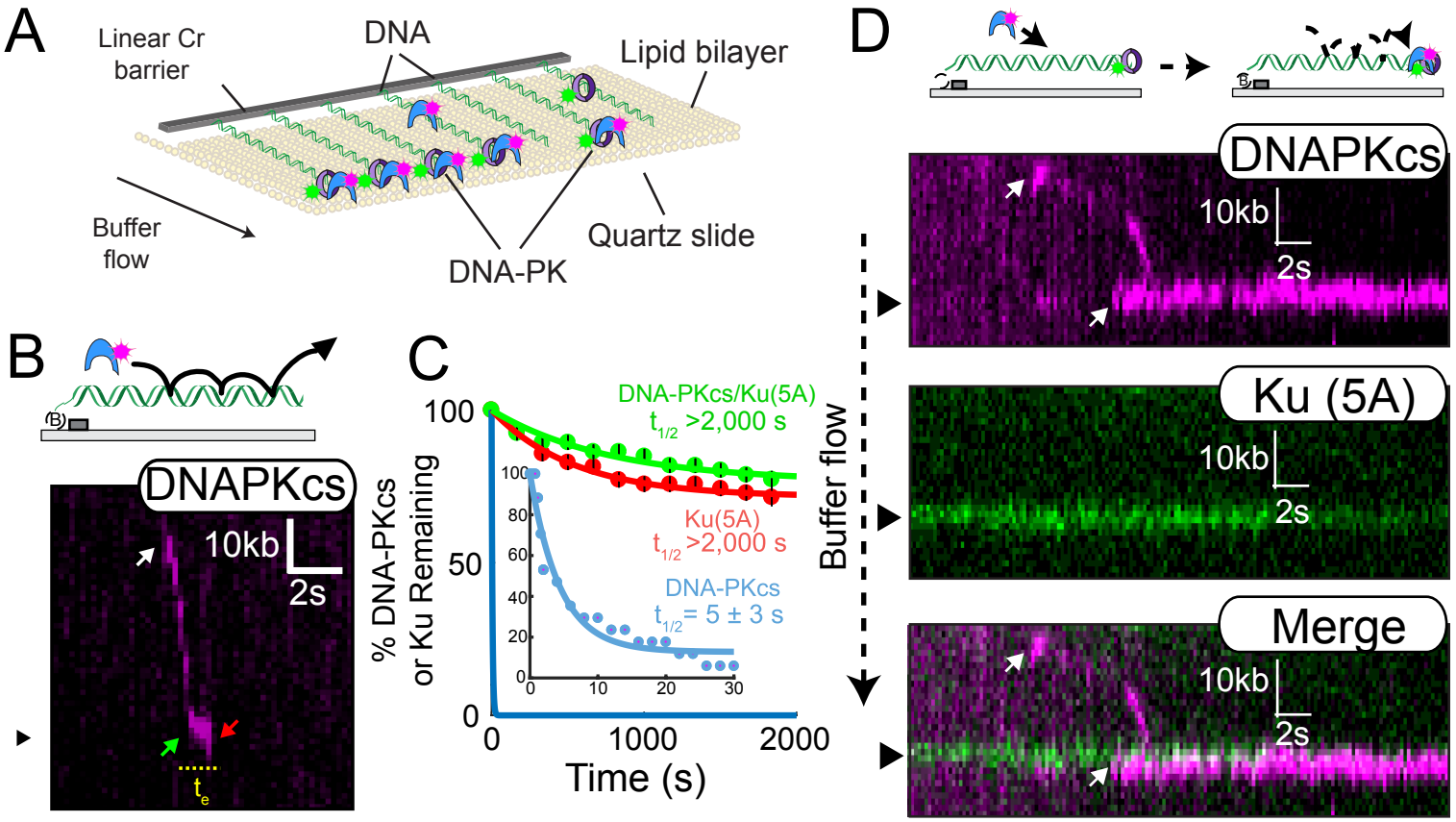

Figure 4

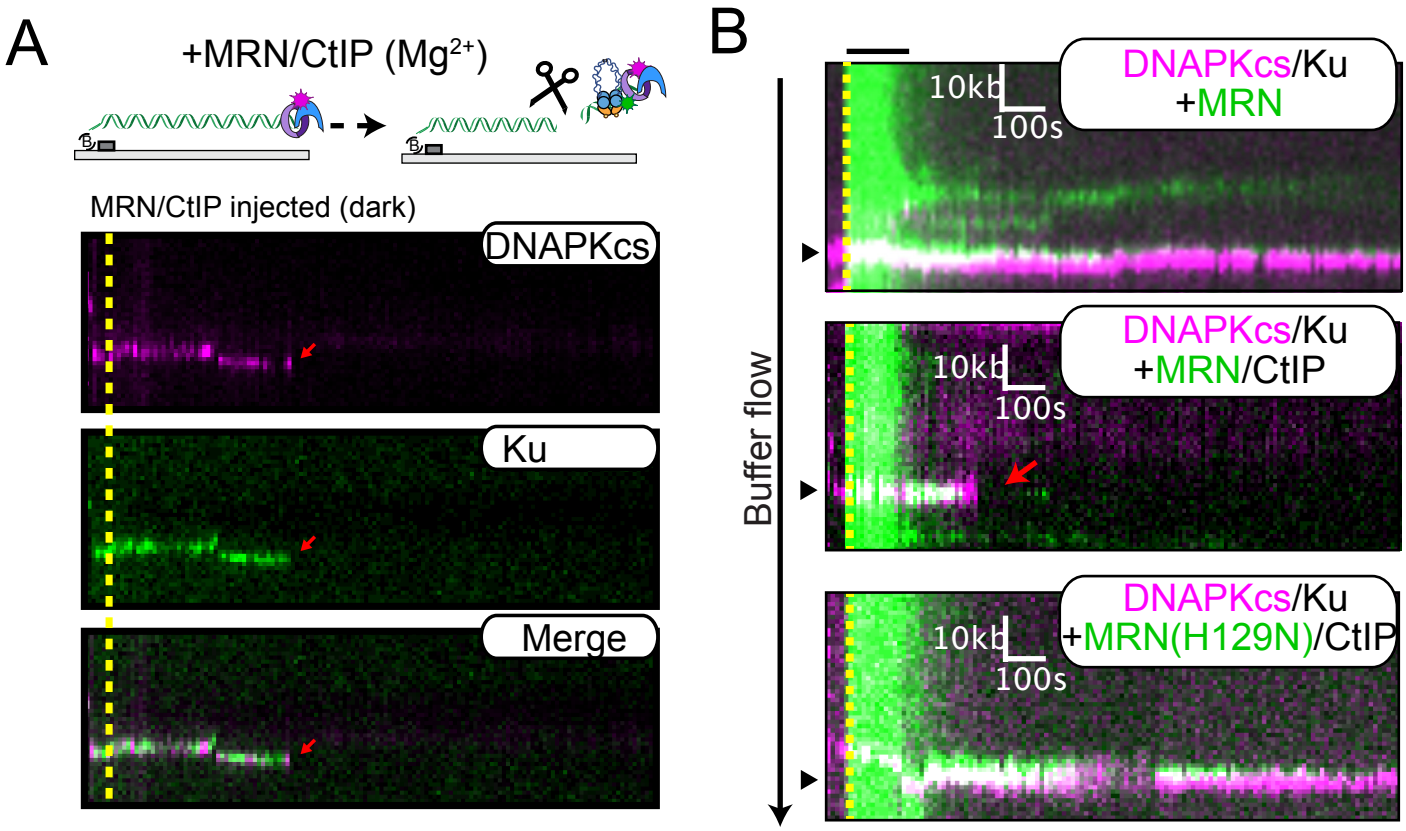

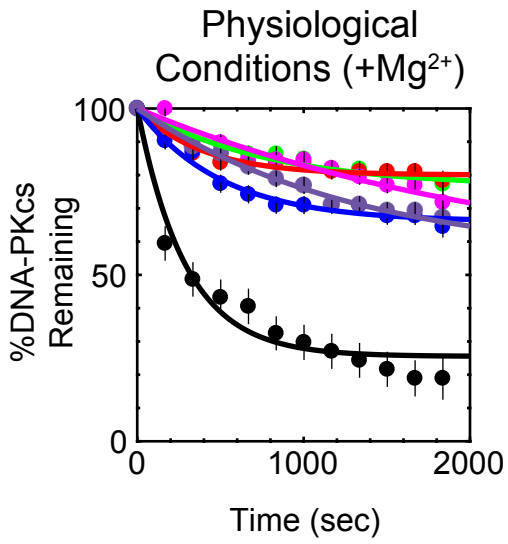

Condition (+Mg^{2+})	DNAPKcs Half-life (sec)	N
DNA-PK	>2,000	66
+MRN/CtIP	324 ± 15	37
+MRN only	>2,000	37
+MRN(H129N)/ CtIP	>2,000	39
+CtIP only	>2,000	31
+MRN/CtIP(AA)	>2,000	52